convergence is obtainable. However, simple conditions in terms of original transition matrices and transition time distributions seem difficult to obtain.

Although iteration of (1) and (2) is thus seen to provide both the infinite horizon solution to the problem and good information as to the decision horizon, the method requires on the order of L times the computation and storage as other available methods (Schweitzer [12] and Morton [7]) for numerically solving the infinite horizon problem. This seems a high price computationally to pay for the additional information. One approximation which might be more attractive would be to replace transition distributions with others with small numbers of nonzero transition probabilities and matching initial distribution moments. For example, it is easy to construct distributions on the integers $1,\cdots,L$ with only four nonzero masses which match the mean and variance of the original distributions, which would make computation more competitive with other schemes, provide the exact infinite horizon solution and at least some decision horizon information. Details are omitted due to space considerations.

ACKNOWLEDGMENT

REFERENCES

[1] J. S. Boyse, "Determining near-optimal policies for Markov renewal decision processes," *IEEE Trans. Syst., Man, Cybern.*, vol. SMC-4, pp. 215–217, Mar. 1974.
[2] G. T. de Ghellinck and G. D. Eppen, "Linear programming solutions for separable Markovian decision problems," *Management Sci.*, vol. 13, pp. 371–394.
[3] N. A. J. Hastings, "Bounds on the gain of a Markov decision process," *Operat. Res.*, vol. 19, pp. 240–244, 1971.
[4] R. A. Howard, *Dynamic Programming and Markov Processes.* Cambridge, Mass.: M.I.T. Press, 1960.
[5] W. S. Jewell, "Markov-renewal programming, I and II," *Operat. Res.*, vol. 11, pp. 938–948, 949–971, 1963.
[6] T. E. Morton, "On the asymptotic convergence rate of cost differences for Markovian decision processes," *Operat. Res.*, vol. 19, pp. 244–249, 1971.
[7] ——, "Undiscounted Markov renewal programming via modified successive approximations," *Operat. Res.*, vol. 19, pp. 1081–1089, 1971.
[8] ——, "The near-myopic nature of the lagged proportional cost inventory problem with lost sales," *Operat. Res.*, vol. 19, 1708–1716, 1971.
[9] A. Odoni, "On finding the maximal gain for Markov decision processes," *Operat. Res.*, vol. 17, pp. 857–860, 1969.
[10] P. J. Schweitzer, "Perturbation theory and Markovian decision processes," M.I.T. Operat. Res. Cent., Tech. Rep. 15, 1965.
[11] ——, "Perturbation theory and undiscounted Markov renewal programming," *Operat. Res.*, vol. 17, pp. 716–727, 1969.
[12] ——, "Iterative solution of the functional equations of undiscounted Markov renewal programming," *J. Math. Anal. Appl.*, vol. 34, pp. 475–501, 1971.
[13] J. L. Smith, "Markov decisions on a partitioned state space," *IEEE Trans. Syst., Man., Cybern.*, vol. SMC-1, pp. 55–60, Jan. 1971.
[14] D. J. White, "Optimal revision periods," *J. Math. Anal. Appl.*, vol. 4, pp. 353–365, 1962.
[15] ——, "Studies in dynamic programming," Ph.D. dissertation, Birmingham Univ., Birmingham, England, 1962.
[16] ——, "Dynamic programming, Markov chains, and the method of successive approximations," *J. Math. Anal. Appl.*, vol. 6, pp. 373–376, 1963.
[17] ——, *Dynamic Programming.* London: Oliver and Boyd, 1969.

A Measure for Circularity of Digital Figures

ROBERT M. HARALICK

Abstract—It is demonstrated that μ_R/σ_R, where R is a random variable of the distance between the center of the figure to any part of its perimeter, is a good measure for the circularity of a digital figure.
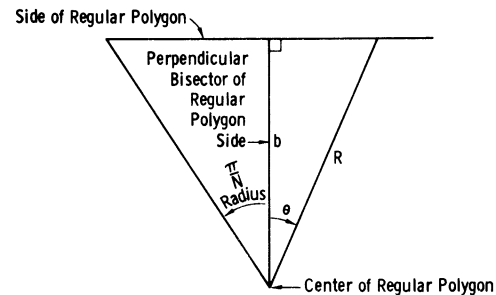
Fig. 1. Geometry of one sector of the N-sided polygon used to compute the density function for R. θ is the angle between the perpendicular bisector of the side, and the radius R. b is the length of the perpendicular bisector.

I. INTRODUCTION

In [1], Rosenfeld has shown that P^2/A, the square of the perimeter of a figure divided by its area, is not a good measure for the dispersedness of digital figures. In fact, depending on how perimeter is defined, the measure P^2/A yields smallest values not for digital circles where it is supposed to, but for digital octagons or diamonds. In this correspondence we suggest a reasonably well-behaved measure for the circularity of digital figures.

A good measure for the circularity of simply closed figures would have the following properties:

1) as a figure becomes more circular, the measure of its circularity increases;
2) the values for digital figures follow the values for the corresponding continuous figures;
3) it is orientation independent;
4) it is area independent.

Let R be a random variable of the distance between the center of a figure and any part of its perimeter. We now show that the measure μ_R/σ_R has these four desirable properties.[1] We do so analytically for properties 1), 3), and 4) and by digital experiments for property 2).

II. ANALYTICAL PROPERTIES OF μ_R/σ_R

To show that as a figure becomes more circular, μ_R/σ_R increases, we must first define a sequence of figures having increasing circularity or compactness. We take for such a sequence the sequence of regular polygons where N, the number of sides, increases in each successive polygon. For each regular polygon of number of sides N, we need to determine the distribution of the radius R so that we can calculate its mean and variance. Without loss of generality, we consider determining the distribution of R for half of one section of a regular polygon. By symmetry, this must also be the distribution for the whole regular polygon. Fig. 1 illustrates the geometry for the polygon: θ is the angle between the perpendicular bisector of the side and the radius R, and b is the length of the perpendicular bisector. Assuming a uniform density for θ over the interval $(0,\pi/N)$, the density for R is

$$f_R(r) = \frac{N}{\pi}\,\frac{b}{r\sqrt{r^2 - b^2}}, \qquad \text{for } b \le r \le \frac{b}{\cos \pi/N}. \quad (1)$$

From this it follows that

$$\mu_R = \frac{Nb}{\pi} \log\left(\frac{1 + \sin \pi/N}{\cos \pi/N}\right) \quad (2)$$

---

[1] This measure is closely related to $V[R]$, which is mentioned by Rosenfeld in [2, p. 162].
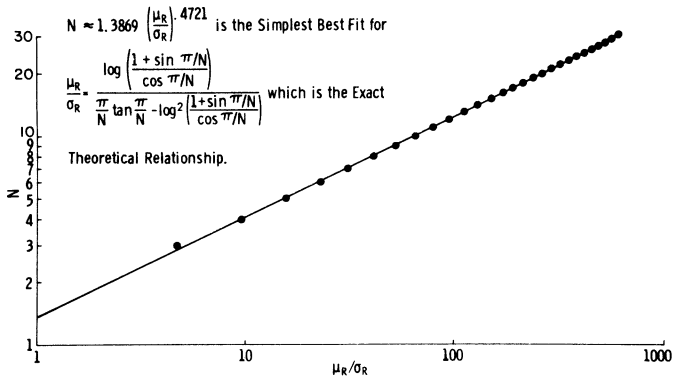
Fig. 2. The dots depict the relationship between μ_R/σ_R and N, the number of sides of the continuous regular polygon. The line is a graph of the best linear fit for the relationship between log N and log μ_R/σ_R.
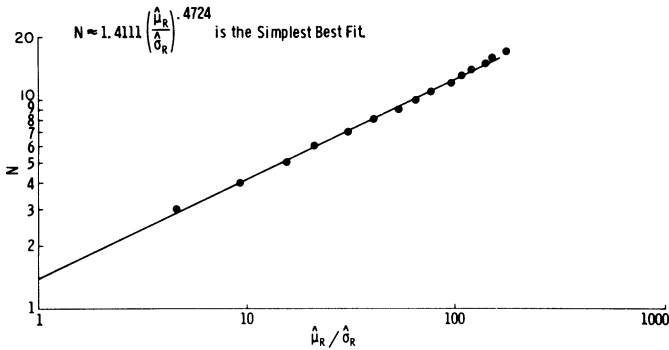
Fig. 3. The 15 dots depict the experimentally determined values relating $\hat{\mu}_R/\hat{\sigma}_R$ and N, the number of sides of a regular digital polygon when the radius of the circumscribed circle for the polygon was near 70 resolution cells. The line is a graph of the best fit linear relationship between log N and log $\hat{\mu}_R/\hat{\sigma}_R$ on the basis of 579 different digital polygons of radius equal to 8 through 70, having number of sides N equal to 3 through $4 + s/5$ and each polygon having random orientation and center.

and that

$$\sigma_R = \left(\frac{Nb}{\pi}\right)\left[\frac{\pi}{N}\tan\frac{\pi}{N} - \log^2\left(\frac{1 + \sin \pi/N}{\cos \pi/N}\right)\right]^{1/2}. \quad (3)$$

The measure μ_R/σ_R then is given by

$$\frac{\mu_R}{\sigma_R} = \frac{\log\left[(1 + \sin \pi/N)/\cos \pi/N\right]}{\{\pi/N \tan \pi/N - \log^2\left[(1 + \sin \pi/N)/\cos \pi/N\right]\}^{1/2}}. \quad (4)$$

Notice that μ_R/σ_R is only a function of N indicating its independence on orientation and area.

Fig. 2 shows a log–log graph of μ_R/σ_R versus N. Clearly μ_R/σ_R not only monotonically increases with N, but the relationship between log N and log μ_R/σ_R is virtually a linear relationship.

The almost linear relationship between log N and log μ_R/σ_R can be demonstrated analytically by determining the Taylor series expansions of $\log^2 ((1 + \sin x)/\cos x)$ and $x \tan x$ around zero. Surprisingly, the first six terms are identical; differences first appear in the seventh and ninth terms. Thus we have for $x = \pi/N$

$$\log (\mu_R/\sigma_R) = -\frac{1}{2} \log \left\{\frac{x \tan x}{\log^2 [(1 + \sin x)/\cos x]} - 1\right\}$$

$$\approx -\frac{1}{2}\log\left\{\frac{x^2 + (x^4/3) + (2x^6/15) + (17x^8/315)}{x^2 + (x^4/3) + (x^6/9) + (53x^8/2520)} - 1\right\}$$

$$\approx -\frac{1}{2} \log 0.02474x^4, \quad \text{for } x \text{ near } \pi/10. \quad (5)$$

Setting $x = \pi/N$ and solving for log N, we obtain

$$\log N \approx \log 1.246 + 0.5 \log (\mu_R/\sigma_R) \quad (6)$$

thereby illustrating the almost linear relationship between log N and log μ_R/σ_R. Solving for the number of sides N, we easily obtain

$$N \approx 1.246(\mu_R/\sigma_R)^{1/2}. \quad (7)$$

In the next section we show that the theoretical best fit relationship and the experimentally determined best fit relationship bear a close resemblance to the analytically determined equation (7).

III. PROPERTIES OF μ_R/σ_R FOR DIGITAL FIGURES

To see how μ_R/σ_R behaved with regular digital polygons, we performed a digital experiment. We generated regular digital polygons from 3 sides to 17 sides of sizes from longest radius of 8 resolution cells to longest radius of 70 resolution cells by the following procedure:

1) for any sized polygon from longest radius s of 8 to longest radius s of 70 and for any polygon whose number of sides N is 3 to a number of sides[2] N is $4 + s/5$;
2) partition a circle of radius s into N equal sectors with the initial sector in arbitrary position and the circle's center in arbitrary position; the radius s and the circle's center are not restricted to be integer valued;
3) for each sector find all resolution cells whose centers are within distance 0.5 (half a resolution cell) of the sector chord;
4) for each resolution cell found, determine its distance R from the center of the figure.
5) compute the mean $\hat{\mu}_R$ and variance $\hat{\sigma}_R^2$ of these distances and from them determine the estimate $(\hat{\mu}_R/\hat{\sigma}_R)$ for μ_R/σ_R.

This procedure produced 579 sample points of N, $(\hat{\mu}_R/\hat{\sigma}_R)$. Taking the natural logarithms of these quantities, the sample points log N, log $(\hat{\mu}_R/\hat{\sigma}_R)$ were used for curve fitting. On the basis of the graphs for the theoretical relationship we expected that log N and log $(\hat{\mu}_R/\hat{\sigma}_R)$ were nearly linearly related and we therefore sought a least square fit for that linear relation. We extended out two-dimensional sample points by adding a third component having constant value 1. To find coefficients vector $a = (a_1,a_2,a_3)$ so that $a'a = 1$ and $\sum_{i=1}^{579} (x_i'a)^2$ is minimized, where x_i is the ith three-dimensional sample point, we found the eigenvector of $\sum_{i=1}^{579} x_ix_i'$ having smallest eigenvalue and set vector a equal to it.[3] The least squares linear fit between log N and log μ_R/σ_R is then given by $x'a = 0$. The smallest eigenvalue divided by the sum of all the eigenvalues indicates the percent variance not accounted for by the least squares linear fit. We found that

$$N = 1.4111 \left[\frac{\hat{\mu}_R}{\hat{\sigma}_R}\right]^{0.4724} \quad (8)$$

was the best least squares fit and that the percent variance accounted for by this fit was over 99 percent. A graph of this fit is presented in Fig. 3. The root mean square error between N and $1.411(\hat{\mu}_R/\hat{\sigma}_R)^{0.4724}$ was 0.3.

In another check of how accurate (8) is in relating $\hat{\mu}_R/\hat{\sigma}_R$ to the integer number of sides N, we compared the nearest integer to $1.411(\hat{\mu}_R/\hat{\sigma}_R)^{0.4724}$ with N the number of sides for each of the 579 regular digital polygons we generated.

For 539 polygons there was no error. For 40 polygons, the error was 1. This represents an identification accuracy of about

[2] We determined that digital polygons generated for a number of sides N greater than $4 + s/5$, where s is the radius of the circumscribed circle for the polygon, were indistinguishable from digital polygons of which the number of sides is $4 + s/5$.

[3] Note that this least squares fit determines the interrelationship between the variables involved. It is not a regression of one variable on the other.

93 percent correct with the 7 percent misidentified polygons having the estimated number of sides off by 1.

For the purpose of comparison, the same least square fit was done with the 15 points $N = 3$ to $N = 17$ used to generate the theoretical graph of μ_R/σ_R, as in (4). Again over 99 percent of the variance was accounted for by the fit, which is given by

$$N = 1.3869 \left[\frac{\mu_R}{\sigma_R}\right]^{0.4721}. \tag{9}$$

For $\mu_R/\sigma_R = 1000$, the difference between the values of N computed with (8) and (9) is less than 1.

IV. CONCLUSION

The results from the digital experiment agree remarkably well with what we expect to happen analytically. Since the digital experiment includes digital regular polygons at many different random sizes, centered randomly in a resolution cell, and at a random angular positions, we can conclude that μ_R/σ_R is a good measure of circularity for both digital and continuous figures.

REFERENCES

[1] A. Rosenfeld, "Compact figures in digital pictures," *IEEE Trans. Syst., Man, Cybern.*, vol. SMC-4, pp. 221–223, Mar. 1974.
[2] ——, *Picture Processing by Computer.* New York: Academic Press, 1969.

On the Medial Axis Function for Visual Patterns

D. J. H. MOORE AND R. A. SEIDL

Abstract—A new version of Blum's medial axial function (MAF) for visual patterns is presented. The new version is incorporated in the chord space analysis framework developed by the authors and has the advantage that, unlike the original version, it is defined for grey level pictures and is a much more "robust" definition. Computer generated examples are shown, and it is indicated how the technique is being applied by the authors in the development of a character recognition system.

I. INTRODUCTION

In a number of recent papers [1], [6] we have presented what we claim to be a fundamental approach to the detection and enhancement of visual pattern features. The approach involves applying a second-order statistical analysis of the pattern—the presence of various types of second- (and more trivially first-) order structure indicating the presence of features. Various techniques for detecting and extracting these features were reported in the aforementioned papers.

The purpose of this correspondence is to point out that the medial axial function (MAF) put forward by Blum [7] can also be incorporated in our mathematical framework. Our version of the MAF is more general than Blum's in the sense that it is defined for grey level pictures[1] and, as will be pointed out, is a
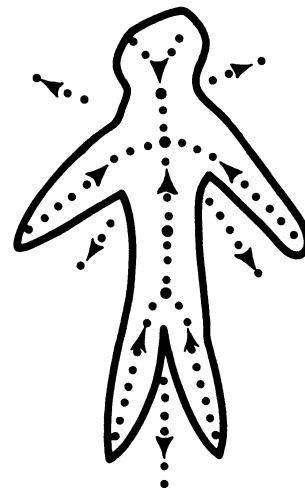
Fig. 1.
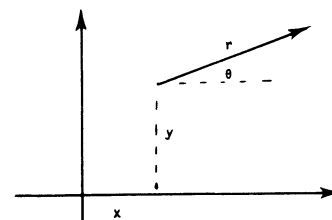
Fig. 2.

more "robust" transformation. The MAF is important for a number of reasons. Blum argues its importance as a general shape descriptor, and there appears to be some evidence that human eye movements are related to the MAF of a line drawing [8], [9]. We are presently involved with incorporating our version of the MAF in a character recognition system where it shows a great deal of promise.

II. MAF AND INTEGRAL GEOMETRY

Blum described a method for which the "skeleton" of a line drawing could be obtained. To define this skeleton, he used an intuitive "grass fire" analogy. The definition leads to an oriented graph (shown dotted in Fig. 1) for line drawings. The graph could be generated by lighting a "grass fire" at time $t = 0$ along the complete contour of the line drawing. The *medial axis* of the pattern (the skeleton) is the locus of where the two or more wave fronts "annihilate" each other.

In our previous work on pattern features, we defined a *chord* as being an oriented line segment, which could be described by the four-tuple (x,y,r,θ) (see Fig. 2).

A chord (x,y,r,θ) belongs to a binary valued pattern p if both endpoints lie on the pattern. The set $\mathscr{C}^*$ of all chords of the pattern can be defined by the characteristic function $f^*(x,y,r,\theta)$ where

$$f^*(x,y,r,\theta) = p(x,y)p(x + r\cos\theta, y + r\sin\theta) \tag{1}$$

where $p(x,y)$ is the binary valued function defining the pattern. $f^*(x,y,r,\theta)$ will be unity for chords belonging to the pattern and zero otherwise.

The existence of second-order structure in the pattern is indicated by nonuniformities in the distribution of the chords $\mathscr{C}^*$ in the *chord space* $\mathscr{U}$ made up of all of the chords in the